Multimodal MFD models: General Formulations and Information Propagation

Mahendra Paipuri, Ludovic Leclercq

Multimodal MFD models: General Formulations and Information Propagation

Mahendra Paipuri & Ludovic Leclercq

Univ. Lyon, IFSTTAR, ENTPE, LICIT, F-69518, Lyon, France
{mahendra.paipuri, ludovic.leclercq}@ifsttar.fr

Manuscript submitted for presentation at the hEART 2019 8th Symposium
Sept. 4–6, 2019, Budapest, Hungary

Word count: 2988 words (excluding the references)
February 26, 2019

Abstract

Traffic state prediction models based on 3D or bi-modal Macroscopic Fundamental Diagram (MFD) is discussed in this work. The well known MFD-based models namely, accumulation-based and trip-based models are extended to the case of multimodal traffic. In addition, accumulation-based with outflow delay, which is studied in the context of link level traffic flow dynamics is investigated. The results from MFD-based models is verified with the solution of continuum space-time model, which is based on hyperbolic conservation equations. It is concluded that accumulation-based model with outflow delay address the limitations of conventional accumulation-based model and trip-based solution is most accurate among all the considered MFD-based models.

1 Introduction

The urban network infrastructure is usually shared by multiple modes like private cars, buses, taxis, bicycles, *etc.*, and each mode has a different impact on the network state dynamics. For instance, previous works (Boyac and Geroliminis, 2011, Chiabaut *et al.*, 2014) suggest that the buses and cars effect the network dynamics in different ways. However, usual MFD-based simulators proposed in the literature employ the so-called single-mode or 2D-MFD, *i.e.*, the relation between density of *all* vehicles and the mean flow of *all* vehicles in the network. Geroliminis *et al.* (2014) is to address this issue and proposed a bi-modal or 3D-MFD for the area of downtown San Francisco based on microsimulations. The 3D-MFD for bi-modal traffic relates the accumulation of cars, buses to the total flow in the network. Ortigosa *et al.* (2015) analyzed the 3D-MFDs of the cities of Zurich and San Francisco using microsimulations to study the effect of dedicated bus lanes on the network performance. The first empirical study of 3D-MFD is proposed by Loder *et al.* (2017) for the city network of Zurich. They had concluded that adding a public transport bus to the network has much more negative impact on the speed of the cars compared to adding a car. More recently, Loder *et al.* (2019) proposed a new functional form for 3D-MFD based on the structure and topology of car and bus network. A single parameter is used to model the interactions between cars and buses. Huang *et al.* (2019) investigated the 3D-MFD using the GPS data of private cars, taxis and public buses for the city of Shenzhen in China. Since, the existence of network level 3D-MFD is evident from recent works, the applicability of this so-called 3D-MFD to the MFD based modeling framework needs to be investigated. Hence, the primary objective of this work is to investigate the MFD-based models formulation founded on a bi-modal or 3D-MFD.

There are primarily two different types of MFD-based models proposed in the literature namely, accumulation-based and trip-based models. Daganzo (2007) proposed the accumulation-based model in the framework of single reservoir system. Despite the fact that accumulation-based is relatively simple to resolve and computationally less demanding, it suffers from few drawbacks as highlighted in Mariotte *et al.* (2017). Hence, trip-based model gained significant attention in the recent past as it can address the issues of accumulation-based model. The idea of trip-based model is proposed by Arnott (2013) and then it is revisited by Leclercq *et al.* (2017), Daganzo and Lehe (2015), Lamotte and Geroliminis (2016). The hypothesis of this approach is that all the vehicles travel at the same speed given by the MFD at a given time and exit the reservoir once they finish the individually assigned trip lengths. Trip-based model can account for the travel time of the vehicles by the virtue of its formulation, however, its computationally more expensive and modeling congestion spill-backs is still a ongoing research question. Recently, Leclercq and Paipuri (2018) showed that no model is perfect and a hybrid model bridging both accumulation-based and trip-based approach gives more consistent results both in free-flow and network saturated regimes.

In this work, both accumulation-based and trip-based models are considered with a bi-modal 3D-MFD. This requires to extend the usual single flow formulation. In addition to traditional MFD-based models, accumulation-based model with outflow delay is proposed. This model is studied in the past (Friesz *et al.*, 1989, Daganzo, 1995, Astarita, 1996) in the context of link level traffic dynamics. This model is revisited in order to address the drawbacks of accumulation-based model and it can be considered as the time-continuous model variant of trip-based framework. Ampountolas *et al.* (2017) used accumulation-based model using 3D-MFD in the context of perimeter control. However, their work focuses on control with fixed composition of bi-modal traffic. This work provides a detailed investigation of MFD-based models founded on 3D-MFD and proposes the appropriate entry and exit flow functions for any composition of traffic states.

2 Functional form of 3D-MFD

For the sake of simplicity, the functional form proposed in Loder *et al.* (2017) is used in the present work. The rationale behind the choice is that this functional form has a clear physical interpretation. The notation of the parameters is adopted from their work. The mean speed of the cars, v_c, can be expressed as a linear function of accumulation of cars, n_c, and accumulation of buses, n_b. The constant of the function, $\beta_{c,0}$, can be treated as the free-flow speed of the cars. Hence, the equation can be expressed as,

$$v_c(n_c, n_b) = \beta_{c,0} + \beta_c\, n_c + \beta_b\, n_b. \tag{1}$$

The coefficients β_c and β_b represent the marginal effect of each mode on the car speeds, *i.e.*, the amount by which the free flow speed of the cars is reduced by adding a vehicle of each mode. On the other hand, the speed of the buses is assumed to be a function of speed of cars. The speed of the buses is given as,

$$v_b(n_c, n_b) = \beta_{b,0} + \beta_{c,b}\, v_c, \tag{2}$$

where $\beta_{c,b}$ is typically less than 1, which shows that the buses travel slower than cars due to frequent stops and $\beta_{b,0}$ accounts for the case of dedicated bus lanes, where buses can travel faster than cars during congestion times. By substituting eq. (1) in eq. (2), it is clear that the mean speed of buses is also an implicit function of n_c and n_b. Now, the total production in the network is sum of the production of cars, P_c, and production of buses, P_b. As the production in the network is defined as product of accumulation and mean speed, the total production can

Table 1: Coefficient values used to compute 3D MFD in the present work.

Cars		Buses	
Coefficient	Value	Coefficient	Value
$\beta_{c,0}$	15	$\beta_{b,0}$	15
β_c	-0.015	$\beta_{c,b}$	0.2
β_b	-0.3		

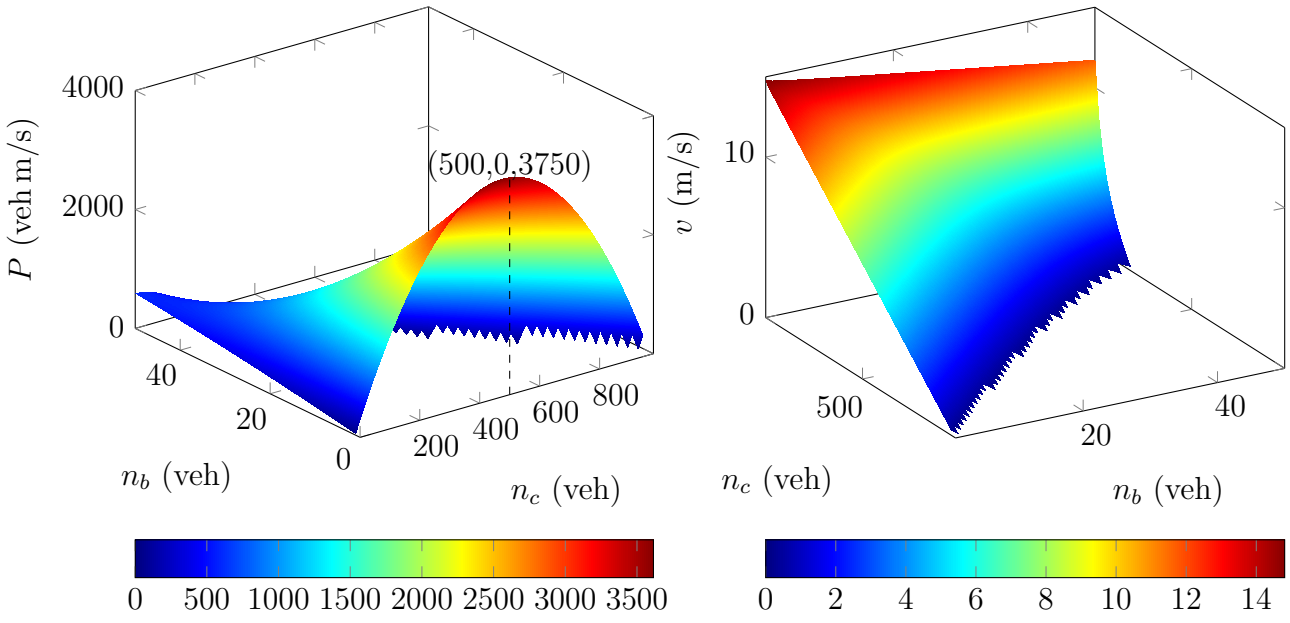

(a) Production MFD surface.

(b) Velocity MFD surface.

Figure 1: Production and velocity 3D-MFD surfaces.

be expressed as,

$$P = n_c\, v_c + n_b\, v_b. \tag{3}$$

From the eq. (3), P can be expressed as $v\,(n_c + n_b)$, where v is the mean speed of all vehicles in the network. Using the definition of total production and eq. (3), the mean vehicular speed in the network can be written as,

$$v = v_c \frac{n_c}{n_c + n_b} + v_b \frac{n_b}{n_c + n_b}. \tag{4}$$

In the work of Loder *et al.* (2017), the calibrated coefficients from Zurich empirical data estimate $\beta_{c,0}$ to be higher than $\beta_{b,0}$, which means that the average free flow speed of cars is higher than average free flow speed of buses. This is due to the fact that buses make frequent stops to aboard and alight the passengers. However, two different free flow speeds for cars and buses results in a sharp gradient close to the origin in velocity MFD surface. This pose problems for numerical scheme of continuum space-time model and hence, in the present work it is assumed that the free flow speed of cars and buses to be the same. However, this assumption can be relaxed for accumulation-based, trip-based and accumulation-based with outflow delay models. Table 1 presents the values of coefficients used in the present work and Fig. 1 shows the production MFD and velocity MFD surfaces obtained. As shown in Fig. 1a, when $n_b = 0$ the critical accumulation of vehicles is 500 and maximum production is $3\,750\,veh\,m/s$. It can be observed that the maximum network production occurs at zero bus accumulation and the maximum production decreases as number of buses increases in the network. Moreover, the critical accumulation, n_{cr}, is not anymore a constant value, but

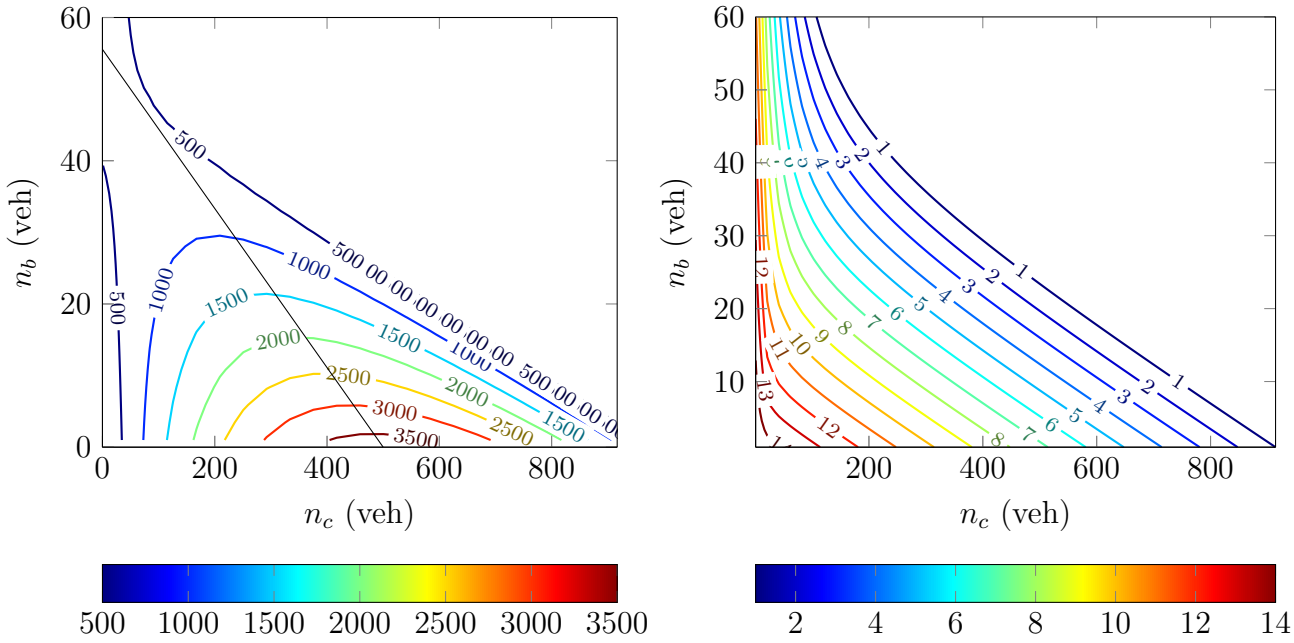

(a) Production MFD contour plot.

(b) Velocity MFD contour plot.

Figure 2: Production and velocity 3D-MFD contour plots.

depends on the partial accumulations of buses and cars in the network. Fig. 2 presents the contour lines for both production and velocity 3D-MFDs. The black line in the production 3D-MFD corresponds to the line of critical accumulation. Mathematically, the equation of the line of critical accumulation can be expressed as $\beta_{c,0} + 2\,\beta_c\,n_c + (\beta_b + \beta_{c,b}\beta_c)\,n_b = 0$.

3 MFD-based models

3.1 Continuum space-time model

The system of hyperbolic conservation equations for each mode, m, can be represented as,

$$\frac{\partial k_m}{\partial t} + \frac{\partial k_m\, v(\mathbf{K})}{\partial x} = 0 \quad \forall\, m, \tag{5}$$

where k_m is the density of mode m and $v(\mathbf{K})$ is the velocity defined by 3D-MFD, which is the function of all densities, *i.e.*, $\mathbf{K} = [k_1, \ldots, k_m]^T$. In the special case of $m = 1$ and flux computed by fundamental diagram, eq. (5) becomes Lighthill–Whitham–Richards (LWR) model (Lighthill and Whitham, 1955, Richards, 1956). The model presented in eq. (5) can be interpreted as multimodal or multiclass traffic flow models. Different multiclass models proposed in literature are well documented in Fan and Work (2015). Since in the present model all vehicles travel at the same speed given by velocity MFD, this model is referred as homogeneous multiclass model. The strict hyperbolicity of the homogeneous multiclass models can be proven when $m \leq 2$ (Benzoni-Gavage and Colombo, 2002, Keyfitz and Kranzer, 1980). System (5) can be re-written as,

$$\frac{\partial \mathbf{K}}{\partial t} + \mathbf{A}\frac{\partial \mathbf{K}}{\partial x} = \mathbf{0}, \tag{6}$$

where $\mathbf{A}$ is the Jacobian matrix and for the present case of $m = 2$ it is given as follows,

$$\mathbf{A} = \begin{bmatrix} v + k_c \frac{\partial v}{\partial k_c} & k_b \frac{\partial v}{\partial k_c} \\ k_c \frac{\partial v}{\partial k_b} & v + k_b \frac{\partial v}{\partial k_b} \end{bmatrix}. \tag{7}$$

It can be shown that the eigen values of the Jacobian $\mathbf{A}$ has real and distinct values if $\frac{\partial v}{\partial k_c} < 0$ and $\frac{\partial v}{\partial k_b} < 0$. The functional form of 3D-MFD is chosen in such a way that this condition is fulfilled.

A single reservoir system with two different trips, one each for cars and buses, is considered in this work. The numerical resolution of the system (5) using MFD as flux function is discussed in-detail in Leclercq *et al.* (2015). Similar approach is used here, albeit, 3D-MFD is used to define the flux function and hence, numerical scheme details are omitted. In brief, the time derivative term is discretized using first-order Euler scheme and the space derivative is discretized using first-order finite volume method. The flux at the cell interface is computed using HLL approximate Riemann solver (Harten *et al.*, 1983). The wave speeds are estimated directly from the maximum and minimum eigen values of the Jacobian matrix in each cell. A constant CFL number of 0.5 is used along with adaptive time stepping scheme in all computations. As stated earlier, the solution of this model is used as reference to compare the accumulation-based, accumulation-based with outflow delay and trip-based results wherever possible.

3.2 Accumulation-based and trip-based models

Essentially, accumulation-based model is the simplification of hyperbolic conservation, where space derivative of flux is neglected. The resulting conservation equation (Daganzo, 2007) to resolve the reservoir dynamics is given as,

$$\frac{\mathrm{d}\, n_m}{\mathrm{d}t} = q_{m,\mathrm{in}}(t) - q_{m,\mathrm{out}}(t) \quad , \ \forall m, \tag{8}$$

where n_m is the space-averaged accumulation in the reservoir for mode m, $q_{m,\mathrm{in}}(t)$ is the total effective inflow and $q_{m,\mathrm{out}}(t)$ is the total effective outflow. The main advantage of this model (8) compared to hyperbolic system (5) is that this system is well-defined for any number of modes, m. As the system (8) comprises of only Ordinary Differential Equations (ODE), the numerical resolution is quite straightforward and simple. On the other hand, accumulation-based model propagates the information with infinite speed, *i.e.*, outflow reacts instantaneously to the changes in the inflow of the reservoir.

The theory of single reservoir and multi-reservoir accumulation-based model is discussed in-detail in Mariotte *et al.* (2017), Mariotte and Leclercq (2018). A first-order forward Euler scheme with a time step, Δt, of 1 sec is used in the present work to numerically resolve accumulation-based model.

Now considering the trip-based formulation, mathematically it can be expressed as,

$$L_m = \int_{t-T_m(t)}^{t} v(n(s))\, \mathrm{d}s \qquad \forall m. \tag{9}$$

Consider $T_m(t)$ is the travel time of a user for mode m who entered the reservoir at time t. The speed at each time instant depends on the total accumulation, n, in the reservoir, which is defined velocity 3D-MFD. Hence, the area under the speed-time curve between the times, $t - T_m(t)$ and t gives the total travel distance, which is trip length L_m. The significant modeling difference in trip-based model compared to accumulation-based model is that the trip-based framework considers the traveled distance explicitly. Hence, the model is more accurate during the transition compared to accumulation-based. Event-based resolution proposed in Mariotte *et al.* (2017) is used in the present work.

3.3 Accumulation-based model with outflow delay

The idea of the accumulation-based model with outflow delay is that the outflow is delayed in the reservoir by the order of the travel time at the time instance, t. Consider vehicles that enter

the reservoir at time, t, has an inflow of $q_{m,\text{in}}(t)$. They leave the reservoir at time, $t+\tau(t)$, where $\tau(t)$ is the travel time inside the reservoir. Under the assumptions of vehicle conservation and FIFO rule, the vehicles that enter at time t must be equal to vehicles that leave the reservoir at time $t + \tau(t)$. Mathematically, it can be expressed as,

$$\int_{-\infty}^{t} q_{m,\text{in}}(s)\,\mathrm{d}s = \int_{-\infty}^{t+\tau(t)} q_{m,\text{out}}(s)\,\mathrm{d}s. \tag{10}$$

Differentiating the eq. (10) with respect to t and rearranging yields,

$$q_{m,\text{out}}(t+\tau(t)) = \frac{q_{m,\text{in}}(t)}{1+\dfrac{\mathrm{d}\tau(t)}{\mathrm{d}t}}. \tag{11}$$

Since, the time derivative of travel time is not known *a priori*, $\dfrac{\mathrm{d}\tau(t)}{\mathrm{d}t}$ can be computed using chain rule as follows,

$$\frac{\mathrm{d}\tau(t)}{\mathrm{d}t} = \sum_m \frac{\mathrm{d}\tau(n_m(t))}{\mathrm{d}n_m}\frac{\mathrm{d}n_m(t)}{\mathrm{d}t} \equiv \sum_m \frac{\mathrm{d}\tau(n_m(t))}{\mathrm{d}n_m}\left(q_{m,\text{in}}(t) - q_{m,\text{out}}(t)\right). \tag{12}$$

The travel time function can be computed from velocity MFD, *i.e.*, $\tau(n_m, n) = \dfrac{L_m}{v(n_m, n)}$. This model ensures that the travel time inside the reservoir is taken into account. From eq. (11), it is evident that the outflow at time $t + \tau(t)$ is non-negative if and only if $\dfrac{\mathrm{d}\tau(t)}{\mathrm{d}t} > -1$. Physically, this restriction translates to strict FIFO behavior inside the reservoir. However, it is already shown in Carey and McCartney (2002) that certain inflow profiles may result in $\dfrac{\mathrm{d}\tau(t)}{\mathrm{d}t} \leq -1$ and hence, violation of FIFO. Daganzo (1995) proved that FIFO is preserved in this model if and only if travel time function is a linear. This can be regarded as a strong restriction in this modeling framework. However, this work addresses this limitation by proposing a weak FIFO discipline. This is achieved by re-arranging the outflow cumulative curve locally whenever there is a violation of FIFO rule.

4 Results and discussion

Firstly, a free-flow scenario is considered to demonstrate the essential differences between different MFD-based models. The trip lengths of cars and buses, L_c and L_b, are assumed to be $\{1050, 2025\}$ m, respectively. 3D-MFD is computed based on the values presented in Table 1. Since the free-flow speeds of cars and buses are assumed to be same, which is generally not the case in real networks, the increase in free-flow speed of buses is compensated by longer trip length. A total simulation time of 10 000 sec is considered with the first 1 000 sec being the warm-up period. A step demand case is assumed for the inflow profile according to following definition,

$$[\lambda_c\ \lambda_b]^T = \begin{cases} [0.1\ 0.01]^T & \text{if } 0 < t \leq 1000 \text{ or } 6000 < t \leq 10000 \\ [1.3\ 0.06]^T & \text{otherwise.} \end{cases} \tag{13}$$

where λ_c and λ_b are the demand for cars and buses in veh/s, respectively. These flows are chosen in such a way that the accumulations of cars and buses stay on the left hand side of the critical accumulation line on the MFD surface shown in Fig. 2a.

Figure 3 shows the evolution of accumulation with time for cars and buses. According to the assumed demand profile (13), there is a sharp increase in the demand at $t = 1\,000$ sec and correspondingly, there is a sharp decrease at $t = 6\,000$ sec. Even though all the models

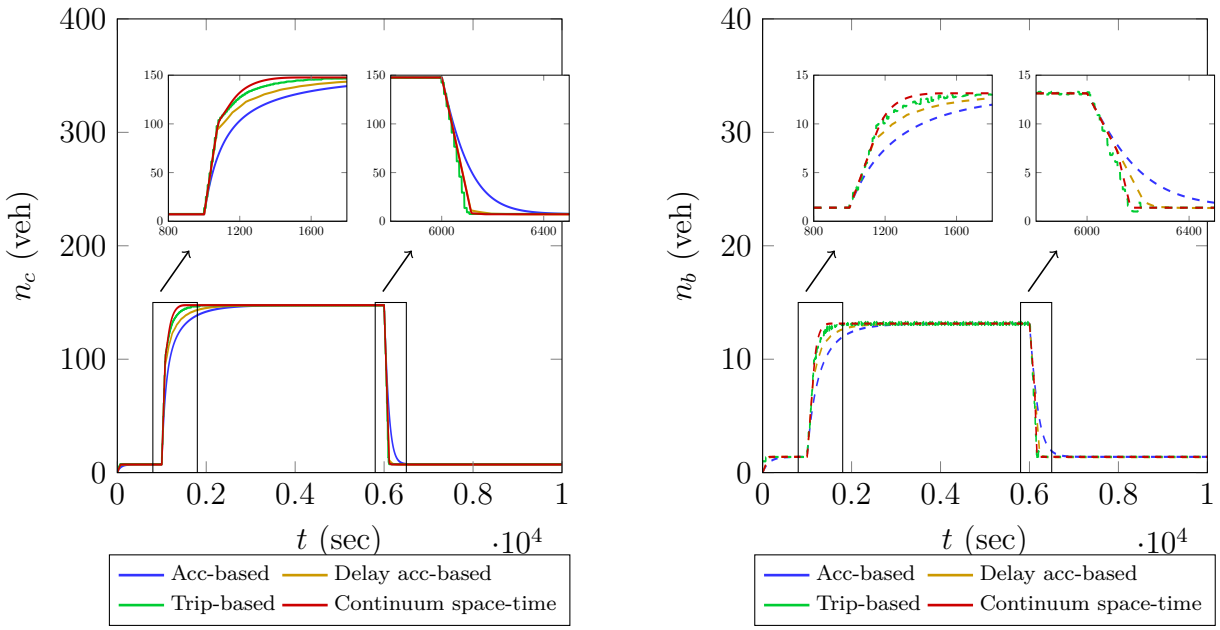

(a) Accumulation *vs.* time for cars. (b) Accumulation *vs.* time for buses.

Figure 3: Evolution of accumulation with time for cars and buses for all MFD-based models considered.

presented in the plots reach the same equilibrium, it is interesting to observe the transition region to evaluate the accuracy of the models. Consider the demand surge at time $t = 1\,000$ sec highlighted in Figs. 3a and 3b. Since the continuum space-time model is the reference solution, it is evident from the plot that trip-based model follows the reference solution more closely following by accumulation-based model with outflow delay and finally, accumulation-based model is least accurate. Since there is no explicit space variation term in the accumulation-based model, only space averaged solution is obtained at each time step and hence, more diffused solution. On the other hand, trip-based model accounts for the wave propagation inside the reservoir to a good accuracy, which can be noticed from the plot. Accumulation-based with outflow delay is in between these two models, *i.e.*, this model cannot account for wave propagation like trip-based, however, the delay in the outflow introduces an average effect of wave propagation. The essential difference between trip-based and accumulation-based with outflow delay is that trip-based can account for the variation of travel time during the trip, whereas delay outflow model cannot account for this variation within the trip. The same applies during the demand drop, *i.e.*, at $t = 6\,000$ sec, albeit, the transition to the equilibrium is rather fast and hence, the differences in models is less obvious. However, the trend can be observed clearly in the cases of buses in Fig. 3b, where trip-based is more accurate and accumulation-based is least accurate.

Figure 4 presents the evolution of outflow with time for different MFD-based models considered. The inflow demand is shown in dotted lines in the plot, where demand surge and drop can be observed. At $t = 1\,000$ sec, it is clear from the plot for both cars and buses, the outflow in the accumulation-based model increases immediately. On contrary, both trip-based model and accumulation-based model with outflow delay produces a sharp increase in the outflow with travel time inside the reservoir considered. In the accumulation-based with outflow delay, a step wise increase in the outflow is observed and this phenomenon is discussed in-detail in Carey and McCartney (2002). Similarly, during the demand drop at $t = 6\,000$ sec, the outflow in the accumulation-based model starts to decrease gradually, whereas trip-based and accumulation-based with outflow delay produces a sharp decrease after accounting the

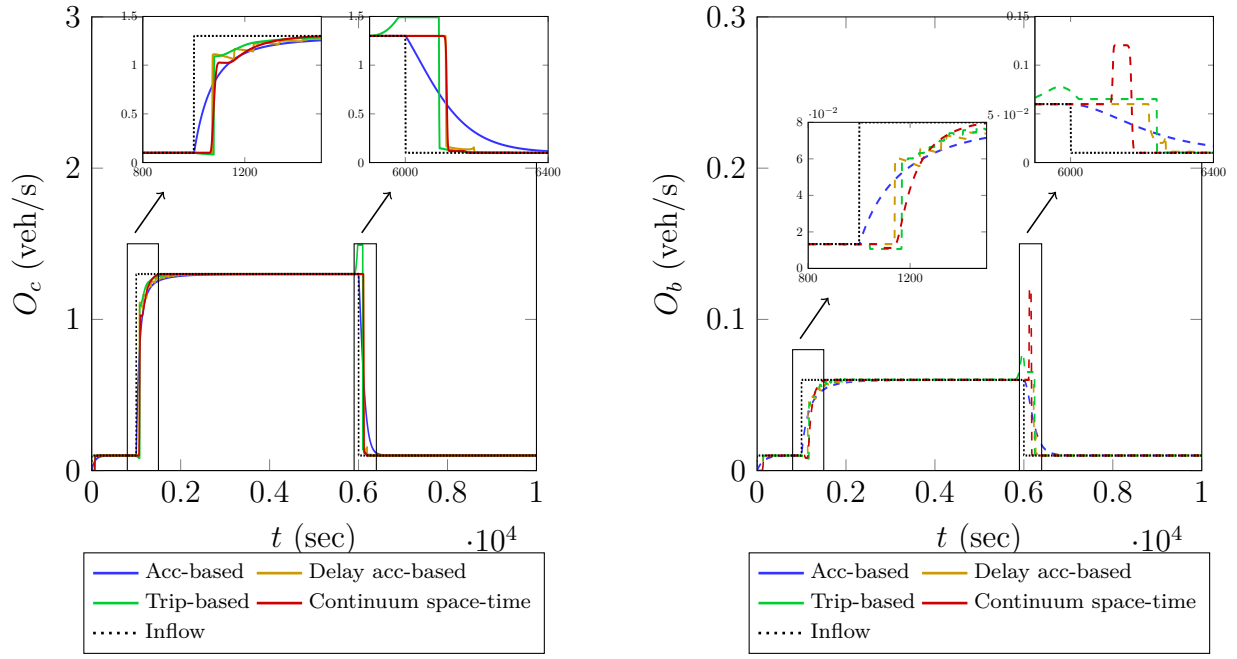

(a) Outflow evolution *vs.* time for cars.

(b) Outflow evolution *vs.* time for buses.

Figure 4: Evolution of outflow with time for cars and buses for all MFD-based models considered.

travel times. An increase in the outflow in trip-based model can be observed just before the demand drop. This is due to the causality effect that is discussed in-detail in Leclercq and Paipuri (2018). Similarly, a small increase in outflow in the buses is noticed at the end of high demand period. This is due to the fact that cars finish their trip faster than buses owing to the smaller trip lengths. Hence, the demand drop occurs in cars sooner than buses, which makes more outflow capacity available for buses and hence, an increase in outflow for buses is noticed. The differences between different models during transition period can be clearly noticed by monitoring the mode share ratio, *i.e.*, ratio of outflow of cars to buses. Fig. 5a presents the mode share ratio evolution with time. During the demand surge, the ratio increases sharply and then converges to the equilibrium state. This sharp increase is due to the fact that the outflow of cars increase prior to the buses (owing to the shorter trip length of cars). Once the outflow of buses reacts to inflow surge, the ratio tends to the equilibrium state. However, accumulation-based model unable to predict this phenomenon.

In conclusion, it is clear that trip-based model is most accurate and accumulation-based is least accurate during the transition period. Interestingly, accumulation-based model with outflow delay partially address the key issues of accumulation-based model and computationally less demanding. The remaining work includes testing the stated modeling frameworks in high demand scenarios. It is noticed that using the conventional entry flow functions with 3D-MFD has unseen consequences. Hence, to address this issue a FIFO disciplined entry flow is proposed. As stated earlier, accumulation-based with outflow delay encounters various issues when modeling congestion inside the reservoir. Those issues are demonstrated and addressed in this work.

Acknowledgment

This project has received funding from the European Research Council (ERC) under the European Union's Horizon 2020 research and innovation program (grant agreement No 646592 –

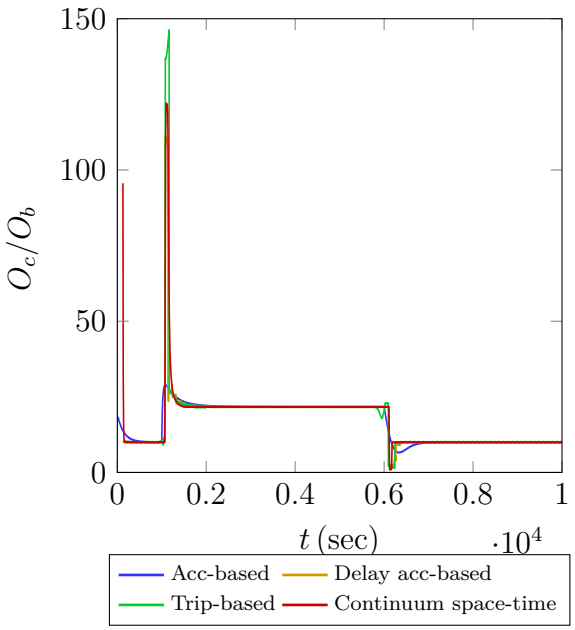

(a) Mode share evolution *vs.* time.

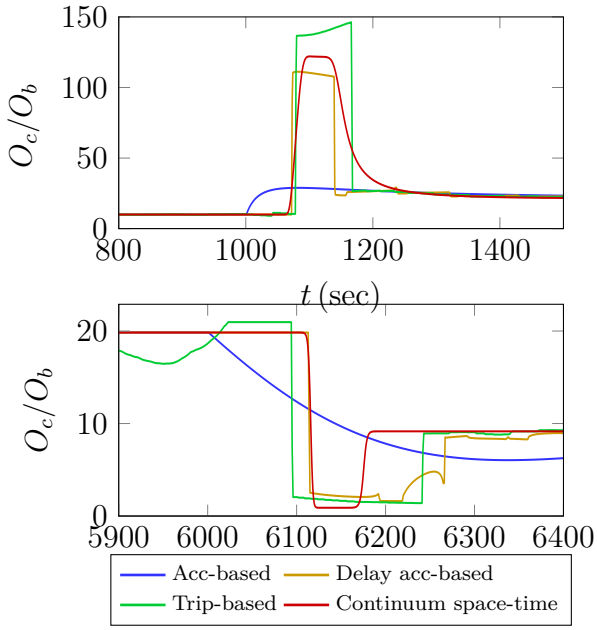

(b) Zoom of mode share at transition periods. Top plot is at demand surge and bottom one is at demand drop.

Figure 5: Evolution of mode share between cars and buses with time for all MFD-based models considered.

MAGnUM project).

References

Ampountolas, K., N. Zheng and N. Geroliminis (2017). Macroscopic modelling and robust control of bi-modal multi-region urban road networks. *Transportation Research Part B: Methodological*, *104*, 616 – 637.

Arnott, R. (2013). A bathtub model of downtown traffic congestion. *Journal of Urban Economics*, *76*, 110 – 121.

Astarita, V. (1996). A continuous time link model for dynamic network loading based on travel time function. In *The 13th International Symposium on Theory of Traffic flow*, 79-102. Lyon.

Benzoni-Gavage, S. and R. M. Colombo (2002). An n-Populations Model for Traffic Flow. *Europ. J. Appl.Math*, *14*, 587–612.

Boyac, B. and N. Geroliminis (2011). Estimation of the network capacity for multimodal urban systems. *Procedia - Social and Behavioral Sciences*, *16*, 803 – 813. 6th International Symposium on Highway Capacity and Quality of Service.

Carey, M. and M. McCartney (2002). Behaviour of a whole-link travel time model used in dynamic traffic assignment. *Transportation Research Part B: Methodological*, *36*(1), 83 – 95.

Chiabaut, N., X. Xie and L. Leclercq (2014). Performance analysis for different designs of a multimodal urban arterial. *Transportmetrica B: Transport Dynamics*, *2*(3), 229–245.

Daganzo, C. F. (1995). Properties of link travel times under dynamic load. *Transportation Research Part B: Methodological*, *29*, 95–98.

Daganzo, C. F. (2007). Urban gridlock: Macroscopic modeling and mitigation approaches. *Transportation Research Part B: Methodological*, *41*(1), 49 – 62.

Daganzo, C. F. and L. J. Lehe (2015). Distance-dependent congestion pricing for downtown zones. *Transportation Research Part B: Methodological*, *75*, 89 – 99.

Fan, S. and D. Work (2015). A heterogeneous multiclass traffic flow model with creeping. *SIAM Journal on Applied Mathematics*, *75*(2), 813–835.

Friesz, T. L., J. Luque, R. L. Tobin and B.-W. Wie (1989). Dynamic network traffic assignment considered as a continuous time optimal control problem. *Operations Research*, *37*(6), 893–901.

Geroliminis, N., N. Zheng and K. Ampountolas (2014). A three-dimensional macroscopic fundamental diagram for mixed bi-modal urban networks. *Transportation Research Part C: Emerging Technologies*, *42*, 168 – 181.

Harten, A., P. Lax and B. Leer (1983). On upstream differencing and Godunov-type schemes for hyperbolic conservation laws. *SIAM Review*, *25*(1), 35–61.

Huang, C., N. Zheng and J. Zhang (2019). Investigation on the bi-modal macroscopic fundamental diagrams in large-scale urban networks - an empirical study of Shenzhen city. In *Transportation Research Board 98rd Annual Meeting Transportation Research Board*, 19-05340. Washington.

Keyfitz, B. L. and H. C. Kranzer (1980). A system of non-strictly hyperbolic conservations laws arising in elasticity theory. *Archives for Rational Mechanics and Analysis*, *72*, 219 – 241.

Lamotte, R. and N. Geroliminis (2016). The morning commute in urban areas: Insights from theory and simulation. In *Transportation Research Board 95th Annual Meeting Transportation Research Board*, 16-2003. Washington.

Leclercq, L. and M. Paipuri (2018). Macroscopic traffic dynamics in reservoirs under fast-varying demand profiles. *Transportation Science*. (Accepted).

Leclercq, L., C. Parzani, V. L. Knoop, J. Amourette and S. P. Hoogendoorn (2015). Macroscopic traffic dynamics with heterogeneous route patterns. *Transportation Research Part C: Emerging Technologies*, *59*, 292 – 307. Special Issue on International Symposium on Transportation and Traffic Theory.

Leclercq, L., A. Sénécat and G. Mariotte (2017). Dynamic macroscopic simulation of on-street parking search: A trip-based approach. *Transportation Research Part B: Methodological*, *101*, 268 – 282.

Lighthill, M. J. and G. B. Whitham (1955). On kinematic waves II. a theory of traffic flow on long crowded roads. *Proceedings of the Royal Society of London. Series A. Mathematical and Physical Sciences*, *229*(1178), 317–345.

Loder, A., L. Ambühl, M. Menendez and K. W. Axhausen (2017). Empirics of multi-modal traffic networks–using the 3D macroscopic fundamental diagram. *Transportation Research Part C: Emerging Technologies*, *82*, 88 – 101.

Loder, A., L. Bressan, I. Dakic, L. Ambühl, M. Bliemer, M. Menendez and K. Axhausen (2019). Modeling multi-modal traffic in cities using the 3D macroscopic fundamental diagram. In *Transportation Research Board 98rd Annual Meeting Transportation Research Board*, 19-03010. Washington.

Mariotte, G. and L. Leclercq (2018). Flow exchanges in multi-reservoir systems with spillbacks. *Transportation Research Part B: Methodological*. (Submitted).

Mariotte, G., L. Leclercq and J. A. Laval (2017). Macroscopic urban dynamics: Analytical and numerical comparisons of existing models. *Transportation Research Part B: Methodological*, *101*, 245 – 267.

Ortigosa, J., N. Zheng, M. Menendez and N. Geroliminis (2015). Analysis of the 3D-vMFDs of the urban networks of Zurich and San Francisco. In *2015 IEEE 18th International Conference on Intelligent Transportation Systems*, pages 113–118.

Richards, P. I. (1956). Shock waves on the highway. *Operations Research*, *4* (1), 42–51.